Lead bromide vapor laser with high repetition rate

G.S. Evtushenko,[1,2] O.V. Zhdaneev,[1,2] A.V. Pavlinsky,[1] V.B. Sukhanov,[1] D.Yu. Shestakov,[1,3] and D.V. Shiyanov[1]

[1] *Institute of Atmospheric Optics, Siberian Branch of the Russian Academy of Sciences, Tomsk*
[2] *Tomsk Polytechnic University*
[3] *Tomsk State University*

Received October 25, 2002

Experimental and theoretical study of lead bromide vapor laser has been carried out at pulse repetition frequency (PRF) of excitation up to 80 kHz. It was found that for a tube with the inner diameter of 1.2 cm and active length of 42 cm mean lasing power is optimal at the PRF of 55–65 kHz. Modeling has shown that at PRF higher than 50 kHz a re-distribution of power taken off from a rectifier takes place. This power is re-distributed between a switch and a gas-discharge tube in favor of the switch that results in worsening both the frequency and power of the laser characteristics. A possibility is experimentally demonstrated of implementing a sealed-off model of lead bromide vapor laser.

Introduction

Pulsed lasers on transitions from resonance level to a metastable one are of great interest because they have high quantum efficiency, mean radiation power, and pulse-repetition frequency. Lead vapor laser was one of the first metal-vapor lasers for which self-terminating lasing has been obtained (on $6p7s^3P_1^0 \rightarrow 6p^2{}^1D_2$ transition of PbI, $\lambda = 722.9$ nm).[1] Then other metal-vapor lasers have been invented. At present the copper vapor and copper bromide vapor lasers have the best output characteristics.[2,3] Because of their high power and operational characteristics, these lasers are widely used in different research areas and technology.[2,4–6] Lead vapor laser is not being applied so widely. One of the reasons for that is short lifetime of an active element associated with carry-over of the working metal from the discharge zone (the carry-over is essentially larger as compared to that in copper vapor laser). At the same time this laser is of some interest because the laser transitions are situated not only in red but also in the violet spectral regions and quantum efficiency on $6p7s^3P_1^0 \rightarrow 6p^2\,{}^1D_2$ transition is the highest for this class of lasers.

A simplified diagram of energy levels and laser transitions for the lead atom is shown in Fig. 1.

To obtain lasing on transitions in the short-wavelength spectral region, the authors of Ref. 7 used pulse cable transformer. In Ref. 8 the mean output power of 4.4 W has been achieved at the wavelength of 722.9 nm and efficiency of 0.1–0.2%. Radiation pulse repetition frequency (PRF) up to 40 kHz has also been realized.[8] In most papers the lead vapor in gas-discharge tube (GDT) has been produced by heating solid lead pieces up to 800–1000°C in active zone. However, there are several papers,[9–11] where volatile molecular lead compounds were used as an active laser material. This allows one to decrease essentially operation temperatures and consequently to simplify design of gas-discharge tubes and in some cases to extend lifetime of the active elements. Thus, Chen[9] put solid $PbCl_2$ into GDT, that was then heated up to 420–560 °C, and obtained lasing at 722.9-nm lead atom line using double pulses. The first pulse was used for dissociation of lead chloride molecules and the second one was used for lead atoms' excitation. Chou and Cool[10] created the $Pb(CH_3)_4$ vapor laser with double pulses and obtained lasing at 722.9 and 406.2-nm lines. Then Feldman with co-authors[11] obtained lasing at red line with the lead iodide vapor laser. Jones and Little[12] used HBr and buffer gas Ne circulation over solid lead pieces. They obtained lasing at 722.9 and 406.2 nm lines at a temperature of 400–500°C in the active zone, thus having realized the so-called hybrid lead vapor laser.

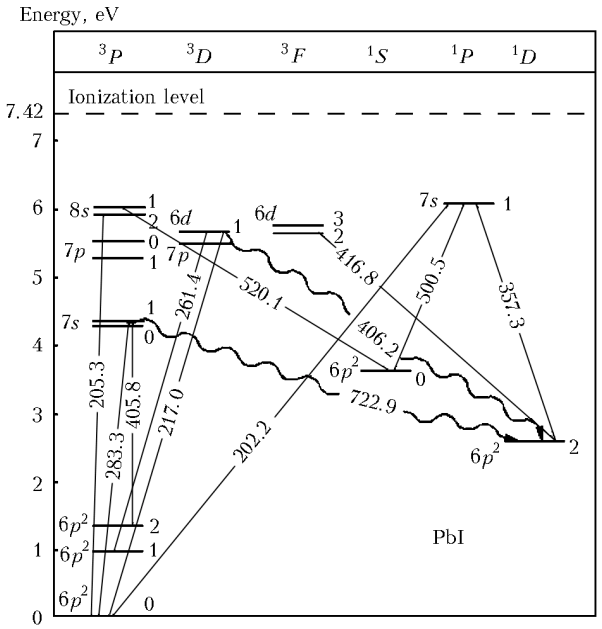

Fig. 1. Simplified diagram of the lead atom energy levels.

0235-6880/03/04 354-05 $02.00

We have formulated a task to make a lead bromide vapor laser without mixture circulation that could be capable of providing a sealed-off mode of operation for an active element.

Experimental setup

The design of an active element of $PbBr_2$ laser under study is typical for metal-halide lasers (Fig. 2*a*), in particular, for CuBr laser. [2, 3]

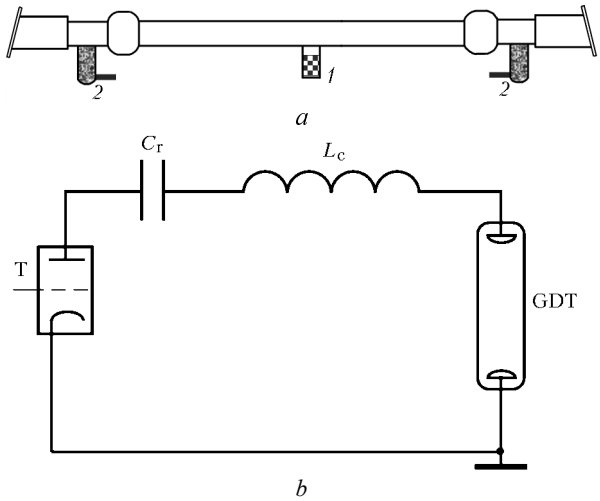

Fig. 2. Design of the gas-discharge tube: (*a*) *1* is a spur with lead bromide heated with an exterior oven, *2* are electrodes; (*b*) is the discharge circuit.

As the operation temperature is lower as compared with pure metal vapor lasers, it is possible to make GDT from fused quartz. To keep the necessary temperature in the working channel, kaolin wool is used as an insulator. Quartz cups filled with copper chips were used as the electrodes *2*. Electric power supply was provided by means of electrodes from IFP-1200 (800) lamps. The spacing between the electrodes was 42 cm, the inner diameter of the channel was 1.2 cm. Solid lead bromide was placed into the special spur *1*, being heated with an external oven, that allowed us to monitor vapor pressure independent of the temperature in the active zone. The buffer gas Ne pressure was varied from 3 to 30 Torr. In some experiments we added a small fraction (up to 0.3 Torr) of hydrogen. Totally reflecting aluminum mirror and plane-parallel quartz plate formed an optical cavity. Lasing lines were identified with an MDR-23 monochromator calibrated against mercury lamp radiation.

Ordinary pumping circuit with direct discharge of reservoir capacitor (C_r) through the GDT and switch[13] (Fig. 2*b*) was used for GDT excitation. Resonance charging of C_r allows one to obtain doubled supply voltage at GDT electrodes. The TGI1-1000/25 thyratron was used as a switch at pulse repetition rate up to 15 kHz. To study the laser characteristics at the increased rates (up to 80 kHz), we applied a tacitron of the TGU1-5/12 type.

Current and voltage pulses were monitored with a S1-122A oscilloscope, the signals to which were applied from Rogowski loop and low-inductance voltage divider. Lasing pulse duration and shape were recorded by means of FK-19 co-axial element. Mean lasing power was measured with IMO-2 and IMO-2N power meters. The chromel-alumel thermocouple was used for monitoring the GDT wall temperature.

Experimental results and discussion

Analysis of radiation spectrum of the discharge in GDT of $PbBr_2$-laser has shown that in the case when an external oven of spur containing lead bromide is off, the neon and hydrogen lines are observed in the radiation spectrum. It is known that hydrogen is always present in gases as uncontrollable admixture, but we did not purify specially the mixture. Besides, we observed in the radiation spectrum much more week lines of admixtures, first of all of copper atom, since GDT electrodes contain copper filings. When heating the spur with lead bromide, lead atomic and ion lines appear in the radiation spectrum (appearance of free lead atoms in the active zone we associate with the electronic dissociation of $PbBr_2$ molecules either directly or through free PbBr radical in discharge). In 10 to 15 minutes after switching the spur heating on, lasing at wavelength of 722.9 and 406.2 nm appeared. Lasing at the violet line is unstable. It is observed in narrow temperature interval and at low neon pressure (units of Torr).

Lasing transitions at 722.9 and 406.2 nm lines have common low level (see Fig. 1). The upper level for the violet line is significantly higher than for the red one, therefore much higher electron energy is needed to populate it efficiently. However even increasing voltage up to 16 kV, we failed to realize stable lasing at the violet line. When adding small hydrogen portions into the tube, the violet line disappears but the red line intensity increases.

Unlike the pure lead vapor laser, in this laser the lasing at the violet line is observed at a more flat leading edge of current pulse and without application of special systems for pumping pulse compression. It is probably connected with the fact that in lead bromide vapor laser more favorable conditions are established for initiating inverse population. It might occur because the low-energy electrons are carried-over from the discharge through their dissociative sticking to Br_2 or HBr molecules at the initial stage of current pulse.

As was mentioned above, to study the laser in a wide frequency range, we used different switches, namely, thyratron from 1 to 12 kHz and tacitron from 30 to 80 kHz. Figure 3*a* presents oscilloscope trace records of voltage and current pulses without metal vapor in the discharge channel and after their input, as well as of the laser pulses at two wavelengths.

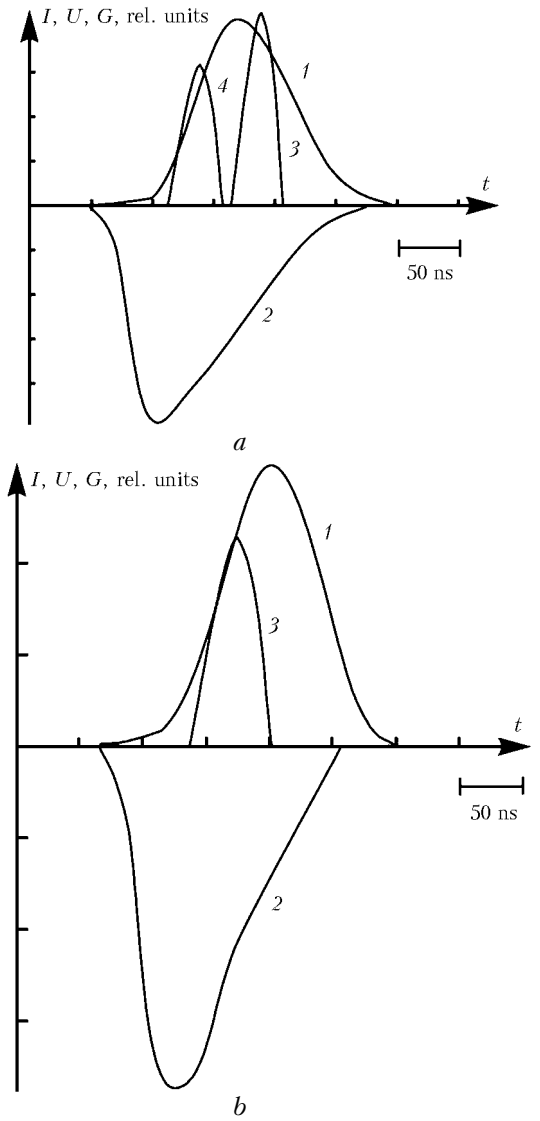

Fig. 3. Oscillograms of current (*1*) and voltage (*2*) pulses, as well as oscillograms of lasing at the red (*3*) and violet (*4*) lines at PRF of 8 (*a*) and 65 kHz (*b*).

Maximum output power of 180 mW at the red line has been achieved with thyratron switch at pumping pulse repetition frequency of 8 kHz and addition of 0.5 Torr of hydrogen. Maximum output power at the red line with tacitron switch achieved 250 mW at pumping PRF of 65 kHz (oscillograms of voltage, current, and lasing emission under these conditions are presented in Fig. 3*b*). To provide lasing at high pumping pulse repetition frequencies and to keep the input power level, it is necessary to decrease the capacitance of the reservoir capacitor. But decreasing reservoir capacitance is limited by the value of the switch self-capacitance (parasitic).

The main mechanisms limiting the service life of the lead vapor laser are the following: carrying-over of the substance from the active zone[2,12] and metal spraying on the inside walls of the tube.[14] We managed to extend service life (up to 100 hours) of the active element of lead bromide vapor laser. It can be explained by lead–bromine atoms' interaction with formation of $PbBr_2$ molecule (similar to metal-halogen cycle in halogen lamps).

It was found during experiments that delay between voltage and current pulses is about 40–50 ns even at high pumping pulse repetition frequency (up to 80 kHz). It is an evidence of low pre-pulse conductivity of the active medium plasma.

Results calculated by a model

Influence of pumping circuit parameters and reagents of gas discharge tube medium on lasing characteristics has been analyzed based on numerical experiments. We have developed a mathematical model on the base of the model for copper vapor laser described earlier in Ref. 15. This mathematical model has two blocks of equations describing parameters of an electrical pumping circuit and parameters of GDT plasma. Time dependence of plasma resistance appears in Kirchhoff equations that can be expressed via time dependences of electron concentration and temperature.

Change of the electron concentration and temperature, in its turn, depends on the current through the GDT and heating electrons. The Kirchhoff equations have the form

$$\frac{\mathrm{d}U_{C_\mathrm{r}}}{\mathrm{d}t} = -\frac{I_\mathrm{r}}{C_\mathrm{r}},$$

$$\frac{\mathrm{d}I_\mathrm{r}}{\mathrm{d}t} = \frac{U_{C_\mathrm{r}} - R_\mathrm{d}(N_\mathrm{e},T_\mathrm{e})I_\mathrm{r} - R_\mathrm{th}(I_\mathrm{r})I_\mathrm{r}}{L_\mathrm{c}},$$

where I_r is the current through the circuit; U_{C_r} is the voltage applied to the reservoir capacitor; $R_\mathrm{d}(N_\mathrm{e}, T_\mathrm{e})$ is plasma resistance; $R_\mathrm{th}(I_\mathrm{r})$ is thyratron resistance; L_c is the circuit inductance. The thyratron resistance has an exponential dependence and within several seconds it decreases from 1 GΩ to units of Ohm.

One can obtain the electron concentration and temperature using the following system of equations:

$$\frac{\mathrm{d}N_\mathrm{e}}{\mathrm{d}t} = k_{\mathrm{i\,Pb}} N_\mathrm{e} N_\mathrm{Pb},$$

$$\frac{\mathrm{d}}{\mathrm{d}t}\left(\frac{3}{2}T_\mathrm{e}N_\mathrm{e}\right) = -Q_\mathrm{i} - Q_{\Delta T} - Q_\mathrm{wall} + Q_j,$$

where $k_{\mathrm{i\,Pb}}$ is the ionization rate of lead atoms[16–19]; T_e is the electrons' temperature;

$$Q_j = \rho(N_\mathrm{e},T_\mathrm{e})j^2(t)$$

is power density transformed into Joule heating; $\rho(N_\mathrm{e},T_\mathrm{e})$ is the specific resistance of plasma;

$$Q_\mathrm{i} = (J_{\mathrm{i\,Pb}}\, k_{\mathrm{i\,Pb}}(T_\mathrm{e})\, N_\mathrm{e}\, [N_\mathrm{Pb} - N_{\mathrm{Pb}^+}]) +$$

$$+ (J_{\mathrm{i\,Ne}}\, k_{\mathrm{i\,Ne}}(T_\mathrm{e})\, N_\mathrm{e}\, [N_\mathrm{Ne} - N_{\mathrm{Ne}^+}])$$

is the power density that is spent on ionization of neon and lead atoms;

$$Q_{\Delta T} = 2\left\{\frac{m_e}{m_{Ne}} k_{Ne} N_{Ne} + \frac{m_e}{m_{Pb}} k_{ei} N_{Pb^+}\right\} N_e \left[T_e - T_{gas}\right]$$

is the power density that is spent on electron cooling due to elastic collisions with buffer gas atoms (neon) and lead ions; N_{Ne}, N_{Pb}, N_{Ne^+}, N_{Pb^+} are concentrations of atoms and ions of the buffer gas (neon) and lead, respectively; k_{Ne} and k_{ei} are the rates of elastic collision of electrons with neon atoms and ions,

$$Q_{wall} = \frac{5.41 \cdot 10^4 T_e^{1.5} N_e}{R^2 \sigma_{e\,Ne} N_{Ne}}$$

is the power density of a heat sink on the walls, in W/cm^3. Here R is a tube radius, in cm; T_e is in eV; $\sigma_{e\,Ne}(T_e)$ is transport collision cross section for elastic collision between electron and neon atom that weekly depends on temperature in the range of 2 eV and it is approximately equal to $1.5 \cdot 10^{-16}$ cm^2;

$$\rho(N_e, T_e) = 0.043\,[a_1(T_e) + a_2(N_e, T_e)]\ (\Omega \cdot \text{cm}),$$

where

$$a_1(T_e) = 4/T_e^{3/2}$$

$$a_2(N_e, T_e) = 7.4 \cdot 10^{-2} N_{Ne} T_e^{3/2}/N_e,$$

a_1 and a_2 are the contributions responsible for the electron–ion and electron–atom collisions, respectively; N_e is the concentration of electrons, in cm^{-3}. It follows from the plasma quasi-neutrality that $N_e = N_{Pb^+} + N_{Ne^+}$.

We did not consider the balance equation for gas temperature because the integration time in equations does not exceed inter-pulse interval during which gas temperature practically does not change.

The system of equations was solved using Gear algorithm for solving stiff set of differential equations.

Typical time dependences of electron temperature and concentration are shown in Fig. 4.

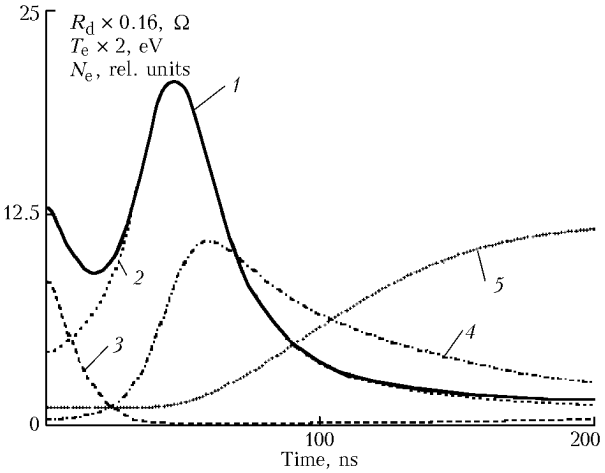

Fig. 4. Calculated time dependences of plasma resistance: general (*1*), accounting only electron–atom collisions (*2*), accounting only electron–ion collisions (*3*); electron temperature (*4*); change of the electron concentration relative to the initial one (*5*).

Having these data, one can simulate time dependence of the GDT resistance. Nonmonotonic behavior of the resistance is associated with the contributions from electron–atom and electron–ion collisions presented in Fig. 4 to total resistance. Moreover it is necessary to note that at the pumping pulse start, the contribution from coulomb electron–ion collisions dominates (see Fig. 4).

Figure 5 presents simulated time dependences of the power input to active laser medium, as well as powers spent on ionization of neon and lead atoms and on gas heating due to elastic collisions.

It is seen that lead atoms ionization is considerable, whereas neon atoms are insignificantly ionized. One might also say that major ionization occurs still as current increases.

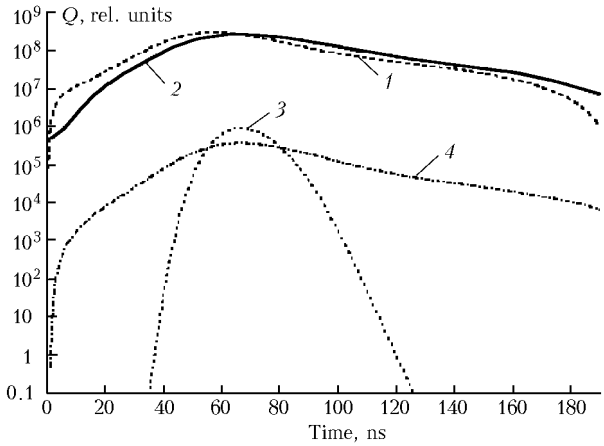

Fig. 5. Time dependences of power deposit into the GDT plasma (*1*), power spent on lead ionization (*2*), power spent on neon ionization (*3*), power spent on gas heating due to elastic collisions (*4*).

Comparison of experimental and simulated time dependences of the GDT current and voltage has shown their satisfactory agreement.

Based on the simulations performed, it was found that there exists optimal lead vapor concentration, at which the most favorable excitation conditions are observed (decrease of leading edges of current and voltage pulses). This is true for both GDT current and voltage. Under these conditions one can expect maximum value of lasing power. As circuit and GDT inductance increase (in simulation they were considered as the total value), the excitation conditions worsen (excitation pulses delay). High pre-pulse electron concentration results in re-distribution of the power taken off from the rectifier between the switch and gas-discharge tube in favor of the switch that can result in worsening both frequency and power laser characteristics.[20]

Conclusion

Stable lead bromide vapor laser operation has been realized at pumping pulse repetition frequency up to 80 kHz. It follows from the experiments that for the tube with 1.2 cm inner diameter and 42 cm

long active zone, mean lasing power has optimum at pumping pulse repetition frequency of 55–65 kHz. It is a bit higher than for CuBr laser having similar diameter.

The model calculations evidence that at pumping pulse repetition frequency higher than 50 kHz, in real pumping circuits of $PbBr_2$ laser, a re-distribution of power taken off from a rectifier takes place due to high pre-pulse electron concentration. This power is re-distributed between a switch and a gas-discharge tube in favor of the switch. This results in worsening both frequency and power characteristics of $PbBr_2$ laser as it happens for copper vapor laser.[20]

A possibility is experimentally demonstrated of implementing a sealed-off model of lead bromide vapor laser with the service life no less than 100 hours.

References

1. G.R. Fowles and W.T. Silfvast, Appl. Phys. Lett. **6**, No. 12, 236–237 (1965).
2. C.E. Little, *Metal Vapor Lasers: Physics, Engineering & Applications* (John Wiley & Sons Ltd, Chichester, UK, 1998), 620 pp.
3. V.M. Batenin, V.V. Buchanov, M.A. Kazaryan, I.I. Klimovsky, and E.I. Molodykh, *Metal Vapor Self-terminating Lasers* (Nauchnaya Kniga, Moscow, 1998), 544 pp.
4. A.N. Soldatov and V.I. Solomonov, *Gas-discharge Lasers on Self-terminated Transitions in Metal Vapor* (Nauka, Novosibirsk, 1985), 152 pp.
5. C. Webb, Proc. SPIE 4**184**, 183–190 (2001).
6. G.S. Evtushenko and V.M. Klimkin, Atmos. Oceanic Opt. **12**, No. 9, 840–848 (1999).
7. A.A. Isaev and G.G. Petrash, Pis'ma Zh. Eksp. Teor. Fiz. **10**, No. 6,188–192 (1969).
8. V.D. Divin and V.K. Isakov, Kvant. Elektron. **13**, No. 8, 1657–1664 (1986.).
9. J.C. Chen, Appl. Phys. Lett**. 45**, No. 10, 4663–4664 (1974).
10. M.S. Chou and T.A. Cool, J. Appl. Phys. **47**, No. 3, 1055–1061 (1976).
11. D.W. Feldman, C.S. Liu, J.L. Pack, and L.A. Weaver, J. Appl. Phys. **49**, No. 7, 3679–3683 (1978).
12. D.R. Jones and C.E. Little, IEEE J. Quantum Electron. **28**, No. 3, 590–593 (1992).
13. G.S. Evtushenko, G.G. Petrash, V.B. Sukhanov, and V.F. Fedorov, Kvant. Elektron. **28**, No. 3, 220–222 (1999).
14. V.M. Klimkin, "*Problems of instability of longitudinal pulse-periodic discharges in metal vapor lasers*," Preprint No. 1, Institute of Atmospheric Optics SB RAS, Tomsk (1999), pp. 1–25.
15. A.M. Boichenko, G.S. Evtushenko, S.I. Yakovlenko, and O.V. Zhdaneev, Laser Physics **11**, No. 5, 580–588 (2001).
16. I.S. Aleksakhin, A.A. Borovik, V.P. Starodub, and I.I. Shafran'onsh, Opt. Spektrosk. **46**, No. 6, 1125–1129 (1979).
17. K. Bartschat, J. Phys. B **18**, No. 8, 2519–2524 (1985).
18. R.S. Freund, R.C. Wetzel, R.J. Shul, and T.R. Hayes, Phys. Rev. A **41**, No. 7, 3575–3595 (1990).
19. V.I. Derzhiev, A.G. Zhidkov, and S.I. Yakovlenko, *Radiation of Ions in Nonequilibrium Dense Plasma* (Energoatomizdat, Moscow, 1986), 160 pp.
20. G.S. Evtushenko and O.V. Zhdaneev, in: *Proc. of VI Int. Conf. on Atomic and Molecular Pulsed Laser* (Institute of Atmospheric Optics SB RAS, Tomsk, 2001), p. 118.